CHIMIE PARIS – PROJETS NUMÉRIQUES

Mobilité différentielle négative dans un milieu encombré

Contact : pierre.illien@sorbonne-universite.fr

Caractériser la réponse d'une particule soumise à une force extérieure dans un environnement encombré qui entrave son déplacement est un problème central de la physique hors-équilibre. Dans le régime de réponse linéaire (où la force est faible), la vitesse de la particule est proportionnelle à la force appliquée. Mais au-delà du régime linéaire, la vitesse de la particule peut présenter certaines caractéristiques anormales. En particulier, il a été observé dans différents contextes (transport d'électrons dans les semi-conducteurs, colloïdes soumis à un champ extérieur...) que la vitesse pouvait être une fonction non-monotone de la force appliquée, et donc que la vitesse du traceur pouvait être une fonction décroissante de la force. On se propose d'étudier ce comportement contre-intuitif en simulant un modèle de gaz sur réseau avec interactions de coeur dur à l'aide d'un algorithme de Monte Carlo cinétique. On mesurera la vitesse du traceur en fonction de la force appliquée, et on déterminera le domaine de paramètres dans lequel il est possible d'observer les comportements contre-intuitifs caractéristiques du régime non-linéaire.

Ce projet est en partie basé sur l'article joint [Phys. Rev. Lett. **113**, 268002 (2014)], qu'il est recommandé de lire avant de commencer.

1 Modèle

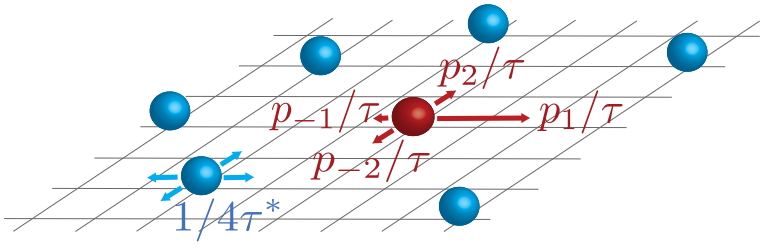

FIGURE 1 – Schéma du modèle de la "diffusion en file". Le traceur est représenté en rouge,

Les particules sont placées sur une réseau carré à deux dimensions et sautent vers les sites voisins avec la contrainte qu'il ne peut y avoir qu'une seule particule par site. On considère le cas général où le traceur peut avoir une fréquence de saut différente de celle des particules constituant son environnement, et où le traceur peut-être soumis à une force extérieure $\boldsymbol{F}$ qui dévie son mouvement dans une direction privilégiée. Plus précisément, le traceur saute dans la direction $\boldsymbol{e}_\mu$ avec une fréquence $k_\mu = p_\mu/\tau$, où la probabilité de saut p_μ est donnée par $p_\mu = C\exp\big(\boldsymbol{F}\cdot\boldsymbol{e}_\mu\big)$, où C est une constante de normalisation à déterminer. Pour fixer les idées, on supposera que la force $\boldsymbol{F}$ est orientée suivant $+\boldsymbol{e}_1$ ($\boldsymbol{F} = F\boldsymbol{e}_1$ avec $F > 0$). Les particules qui constituent le bain sautent dans une des 4 directions possibles avec une fréquence $k = 1/(4\tau^*)$. Dans chaque cas, les sauts ne sont possibles que si le site cible est libre.

On note $\boldsymbol{R}(t) = (X(t), Y(t))$ le site occupé par le traceur à l'instant t. Initialement, on prend $\boldsymbol{R}(0) = 0$ (i.e. le traceur occupe le site 0) tandis que chacun des autres sites est initialement occupé avec une probabilité $0 \leq \rho \leq 1$, qui représente la densité de particules sur le réseau.

2 Implémentation

La dynamique du système est représentée en temps continu : on suppose que chaque particule porte une "horloge" qui sonne à des temps espacés aléatoirement et distribués selon une loi exponentielle (de moyenne τ pour le traceur et de moyenne τ^* pour les particules du bain). A chaque sonnerie de l'horloge, la particule décide de sauter à droite ou à gauche, et le saut est réalisé si le site cible est libre.

L'algorithme de Gillespie (ou Monte Carlo cinétique) permet de simuler une telle dynamique. L'algorithme est décrit par exemple sur la page wikipedia : `https://en.wikipedia.org/wiki/Kinetic_Monte_Carlo`.

On construira un réseau de $L \times L$ sites (numérotés de $(0,0)$ à $(L-1, L-1)$) avec des conditions aux limites périodiques. On appelle $\boldsymbol{r}(t) = (x(t), y(t)) = \boldsymbol{R}(t) - \boldsymbol{R}(0)$ le déplacement du traceur à l'instant t. L'objectif de la simulation est d'obtenir en sortie un tableau de la forme suivante :

t	$\langle x(t)\rangle$	$\langle y(t)\rangle$	$\langle x(t)^2\rangle$	$\langle y(t)^2\rangle$
...	...	...	...	...

où $\langle \ldots \rangle$ désigne une moyenne sur les conditions initiales et sur l'évolution aléatoire du système une fois que la condition initiale a été prescrite.

3 Observations

1. **Vitesse du traceur.** Mesurer pour différents jeux de paramètres la vitesse du traceur selon la direction x du réseau, définie comme $V = \lim_{t\to\infty} \langle x(t)\rangle / t$.
2. **Mobilité différentielle négative.** Tracer la vitesse du traceur en fonction de la force F pour plusieurs valeurs du paramètre τ^*. Qu'observe-t-on ? Comment expliquer physiquement ce comportement ?
3. **Argument qualitatif.** Comprendre le raisonnement permettant de mener à l'équation (2) du papier joint, et comparer cette expression qualitative aux observations numériques.

4 Pour aller plus loin

1. Calculer le coefficient de diffusion du traceur dans la direction du biais, défini comme

$$D = \lim_{t\to\infty} \frac{\langle x(t)^2\rangle - \langle x(t)\rangle^2}{4t} \tag{1}$$

   Comment D dépend-il de la densité de particules sur le réseau ?

2. On définit la variable aléatoire $\eta_{\boldsymbol{u}}(t)$, qui vaut 0 si le site $\boldsymbol{u}$ est vide à l'instant t et 1 s'il est occupé (on prend pour convention $\eta_{\boldsymbol{R}(t)} = 0$). On définit $\phi(\boldsymbol{u}, t) = \langle \eta_{RR(t)+\boldsymbol{u}}(t)\rangle$. Que représente $\phi(\boldsymbol{u}, t)$ physiquement ? Tracer $\phi(\boldsymbol{u} = x\boldsymbol{e}_1, t)$ pour différents paramètres et à différents temps. Comment dépendent-elles de x ?

Microscopic Theory for Negative Differential Mobility in Crowded Environments

O. Bénichou, P. Illien, G. Oshanin, A. Sarracino, and R. Voituriez
Sorbonne Universités, UPMC Univ Paris 06, UMR 7600, LPTMC, F-75005 Paris, France and CNRS, UMR 7600, Laboratoire de Physique Théorique de la Matiére Condensée, F-75005 Paris, France
(Received 18 July 2014; published 31 December 2014)

We study the behavior of the stationary velocity of a driven particle in an environment of mobile hard-core obstacles. Based on a lattice gas model, we demonstrate analytically that the drift velocity can exhibit a nonmonotonic dependence on the applied force, and show quantitatively that such negative differential mobility (NDM), observed in various physical contexts, is controlled by both the density and diffusion time scale of the obstacles. Our study unifies recent numerical and analytical results obtained in specific regimes, and makes it possible to determine analytically the region of the full parameter space where NDM occurs. These results suggest that NDM could be a generic feature of biased (or active) transport in crowded environments.

DOI: 10.1103/PhysRevLett.113.268002 PACS numbers: 83.10.Pp, 05.40.Fb

Introduction.—Quantifying the response of a complex system to an external force is one of the cornerstone problems of statistical mechanics. In the linear response regime, a fundamental result is the fluctuation-dissipation theorem, which relates system response and spontaneous fluctuations. Within recent years a great deal of effort has been devoted to generalizations of this theorem to nonequilibrium situations [1–4], when the time-reversal symmetry is broken, and also to elucidating the effects of the higher order contributions in the external perturbation [5–11]. From the experimental perspective, a theoretical understanding of the latter issues is of utmost importance in several fields, such as active microrheology [12–14] and dynamics of nonequilibrium fluids [15,16].

A striking example of anomalous behavior beyond the linear regime is the negative response of a particle's velocity to an applied force, observed in diverse situations in which a particle subject to an external force F travels through a medium. The terminal drift velocity $V(F)$ attained by the driven particle is then a nonmonotonic function of the force: upon a gradual increase of F, the terminal drift velocity first grows as expected from linear response, reaches a peak value, and eventually decreases. This means that the differential mobility of the driven particle becomes negative for F exceeding a certain threshold value. Such a counterintuitive "getting more from pushing less" [17] behavior of the differential mobility (or of the differential conductivity) has been observed for a variety of physical systems and processes, e.g., for electron transfer in semiconductors at low temperatures [18–21], hopping processes in disordered media [22], transport of electrons in mixtures of atomic gases with reactive collisions [23], far-from-equilibrium quantum spin chains [24], some models of Brownian motors [25,26], soft matter colloidal particles [27], different nonequilibrium systems [17], and also for the kinetically constrained models of glass formers [28–30].

Apart from these examples, negative differential mobility (NDM) has been observed in the minimal model of a driven lattice gas, which captures many essential features of the behavior in realistic systems. In this model, one focuses on the dynamics of a hard-core tracer particle (TP) which performs a random walk of mean waiting time τ, biased by an external force F, on a lattice containing a bath of hard-core particles (or "obstacles") of density ρ, which perform symmetric random walks of mean waiting time τ^*. Such a system may be viewed as the combination of two paradigmatic models of nonequilibrium statistical mechanics, namely the symmetric and asymmetric exclusion processes, which have been extensively studied to describe heat and particle transport properties [31]. Up to now, only limiting situations of this model have been analyzed.

In the case of *immobile* bath particles ($\tau^* \to \infty$), it has been argued that for a tracer subject to an external force and diffusing on an infinite percolation cluster, the drift velocity vanishes for large enough values of the force, and therefore NDM occurs [32]. More recently, NDM was also observed via numerical simulations for low density of immobile particles [33,34] and analytically accounted for [33], but to the first order in ρ only. Surprisingly enough, it appears that NDM is not a specific feature of a frozen distribution of obstacles but also emerges in dynamical environments undergoing continuous reshuffling due to obstacles random motion ($\tau^* < \infty$). Indeed, very recently, numerical analysis performed in [35] at a specific value of the density revealed that NDM could occur in a 2D driven lattice gas for bath particles diffusing slowly enough.

In general, the origin of the NDM has been attributed to the nonequilibrium (called "frenetic") contributions appearing in the fluctuation-dissipation relation [36,37]. As shown earlier in Refs. [38,39], due to its interactions with the environment, the TP drives such a crowded system to a nonequilibrium steady state with a nonhomogeneous

obstacle density profile. However, the nonequilibrium condition is clearly not the only necessary condition for the NDM to emerge—in simulations in [35] this phenomenon is apparent for some range of parameters but it definitely should be absent when the obstacles move sufficiently fast that the TP sees the environment as a fluid.

Finally, NDM seems to be controlled by both the density ρ and the diffusion time scale τ^* of the bath particles. However, a microscopic theoretical analysis of this effect is still lacking. The only available analysis is restricted to the case of immobile obstacles (in the low-density regime) where, by definition, the bath particles are not perturbed by the TP. In this Letter, we reveal the complete scenario of this coupled dynamics providing (i) a scaling argument in the dilute regime that unveils the physical mechanism of NDM, (ii) an analytic analysis of the TP velocity for arbitrary values of system parameters, and (iii) a criterion for the NDM effect to be observed, which shows in particular that for any ρ NDM exists if τ^* is large enough (see Fig. 1).

More precisely, using a decoupling of relevant correlation functions, we derive the force-velocity relation $V(F)$ valid for general ρ, τ, τ^*, and F, and for any dimension $d \geq 2$. This approximate expression is shown to be exact both in the dilute and in the dense limit and provides results in excellent agreement with numerical simulations for a wide range of parameters. In the low-density regime, we recover the exact result obtained in Ref. [33] in the limit $\rho \to 0$ and $\tau^* \to \infty$, while in the high-density limit our general expression gives back the exact results of [40]. Therefore, our theoretical framework unifies existing asymptotic results [33–35]. Our analytic result also allows us to quantify the nontrivial nonmonotonic behavior of the velocity with respect to the force, bringing to the fore the central role of the coupling between density and time

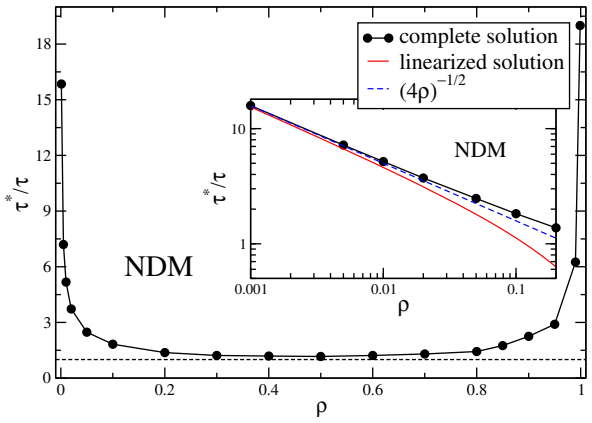

FIG. 1 (color online). Region of negative differential mobility (NDM) in the plane τ^*/τ vs ρ, for $d = 2$ (black circles), as revealed by our analytical approach. Inset: zoom of the low-density region and comparison with the prediction of the linear approximation, Eq. (7) (red line), and with asymptotic result, Eq. (5) (blue dashed line).

scales. In particular, we analytically determine in the plane $(\rho, \tau^*/\tau)$ the region for NDM and establish an accurate criterion for the existence of the NDM (exact at linear order in ρ); see Fig. 1 [41].

Model.—The dynamics in the system under study is defined as follows. Each bath particle, selected at random, waits an exponential time with mean τ^* and then selects the jump direction with probability $1/2d$. Once the jump direction is chosen, the obstacle attempts to move onto the target site: the move is realized if the target site is empty at this time moment; otherwise, if the target site is occupied by either another obstacle or the TP, the move is rejected. In a similar fashion, the TP waits an exponential time with mean τ and then chooses to jump in the direction ν ($\nu \in \{\pm 1, \ldots, \pm d\}$) with probability

$$p_\nu = \frac{e^{(\beta/2)\boldsymbol{F}\cdot\boldsymbol{e}_\nu}}{\sum_\mu e^{(\beta/2)\boldsymbol{F}\cdot\boldsymbol{e}_\mu}}, \tag{1}$$

where β is the inverse temperature (measured in the units of the Boltzmann constant), $\boldsymbol{e}_\mu$ are the corresponding $2d$ base vectors of the hypercubic lattice, the lattice step has been taken equal to 1, and we denote $\boldsymbol{F} \equiv F\boldsymbol{e}_1$. Note that Eq. (1) provides the standard choice of the transition probabilities, which satisfy the generalized detailed balance condition [42], but arbitrary choices of p_ν [35] can be considered within our formalism [43].

Before discussing the mathematical details of our approach, we first present a scaling argument that reveals the physical mechanism underlying NDM and provides an estimation of the threshold in the low-density limit. Assuming a strong external force, one has $p_1 \simeq 1 - \epsilon$, $p_{-1} = \mathcal{O}(\epsilon^2)$, with $\epsilon = 2\exp(-\beta F/2)$, so that the mean velocity in the absence of obstacles can be written $(1-\epsilon)/\tau$. The stationary velocity in the presence of obstacles is then given by the mean distance $1/\rho$ traveled by the TP between two obstacles divided by the mean duration of this excursion, which is the sum of the mean time of free motion $\tau/[\rho(1-\epsilon)]$ and of the mean trapping time τ_{trap} per obstacle. The escape from a trap results from two alternative independent events: the TP steps in the transverse direction (with rate ϵ/τ) or the obstacle steps away [with rate $3/(4\tau^*)$, for $d = 2$]. This leads to $1/\tau_{\text{trap}} = 3/(4\tau^*) + \epsilon/\tau$, and finally

$$V(F) = \frac{1-\epsilon}{\tau + 4\rho(1-\epsilon)\frac{\tau^*}{3+4\epsilon\tau^*/\tau}}. \tag{2}$$

From this formula, it can be seen that V is decreasing with F at large F (i.e., small ϵ), and therefore is nonmonotonic with F, as soon as $\tau^* \gtrsim \tau/\sqrt{\rho}$. This unveils the physical origin of NDM in the dilute regime, where two effects compete. On the one hand, a large force reduces the travel time between two consecutive encounters with bath particles; on the other hand, it increases the escape time from

traps created by surrounding particles. Eventually, for τ^* large enough, such traps are sufficiently long lived to slow down the TP when F is increased. In order to get a rigorous and quantitative understanding of NDM for all parameter values, we now analyze in detail the microscopic dynamics of the model.

General expression of the velocity.—Let the Boolean variable $\eta(\boldsymbol{R}) = \{1, 0\}$ denote the instantaneous occupation of the site at position $\boldsymbol{R}$ by any of the obstacles, $\eta \equiv \{\eta(\boldsymbol{R})\}$ denote the instantaneous configuration of all such occupation variables, and $\boldsymbol{R}_{\rm TP}$ the instantaneous position of the driven particle. The stationary velocity $V(F)$ along the field direction is easily shown to be given by (see the Supplemental Material [44])

$$V(F) \equiv \frac{d\langle \boldsymbol{R}_{\rm TP} \cdot \boldsymbol{e}_1 \rangle}{dt} = \frac{1}{2d\tau^*}(A_1 - A_{-1}), \tag{3}$$

where the coefficients A_ν ($\nu = \pm 1, \ldots, \pm d$) are defined by the relation $A_\nu \equiv 1 + (2d\tau^*/\tau)p_\nu(1 - k(\boldsymbol{e}_\nu))$. Here, $k(\boldsymbol{e}_\nu) \equiv \sum_{\boldsymbol{R}_{\rm TP},\eta} \eta(\boldsymbol{R}_{\rm TP} + \boldsymbol{e}_\nu) P(\boldsymbol{R}_{\rm TP}, \eta)$ represents the stationary density profile around the TP, $P(\boldsymbol{R}_{\rm TP}, \eta)$ being the joint probability of finding the TP at the site $\boldsymbol{R}_{\rm TP}$ with the configuration of obstacles η.

In order to obtain a general expression for the TP stationary velocity for arbitrary force, we make use of the decoupling approximation [46] for the correlation function of the occupation variables of the form

$$\langle \eta(\boldsymbol{R}_{\rm TP} + \boldsymbol{\lambda}) \eta(\boldsymbol{R}_{\rm TP} + \boldsymbol{e}_\nu) \rangle \approx \langle \eta(\boldsymbol{R}_{\rm TP} + \boldsymbol{\lambda}) \rangle \langle \eta(\boldsymbol{R}_{\rm TP} + \boldsymbol{e}_\nu) \rangle, \tag{4}$$

which presumes that the occupation of the site just in front of the TP, and of a site some distance λ apart of it, become statistically independent. This approach represents a mean-field-like approximation and its physical motivation relies on the observation that a fluctuation in the occupancy of the sites in the vicinity of the tracer does not affect the dynamics far from the tracer itself. This decoupling scheme has been previously used in Refs. [38,39] to derive general equations for the TP velocity in two-dimensional open systems. However, the analysis in [38,39] was only concerned with the linear response regime, giving access to the Stokesian behavior of the mobility and hence, via the Einstein relation, to the diffusion coefficient of the particle in the absence of external bias. Here we extend this analysis to nonlinear response (arbitrary force) and arbitrary dimensionality of the embedding lattice in order to define the physical conditions under which the NDM takes place.

Following Ref. [39], this decoupling approximation can be shown to lead to a closed system for the A_ν, which is reported in the Supplemental Material [44]. This system is highly nonlinear in the coefficients A_ν. However, it can be numerically solved to find the analytic value of the TP velocity for an arbitrary choice of the model parameters.

Criterion for NDM.—By using our analytical solution, the region for NDM in the plane $(\rho, \tau^*/\tau)$ can be determined, as reported in Fig. 1, which constitutes the key result of this Letter. Importantly, this shows that for every density there exists a value of τ^*/τ above which NDM can be observed; this value diverges for both $\rho \to 0$ and $\rho \to 1$. In turn, for any value of $\tau^*/\tau \gtrsim 1$, there exists a range of density $[\rho_1, \rho_2]$, for which NDM occurs. When τ^*/τ is sufficiently large, the value of ρ_1 can be made explicit using a small density expansion [see Eqs. (6) and (7)]. This leads to the exact asymptotic result

$$\rho_1 \underset{\tau^*/\tau \to \infty}{\sim} \frac{1}{4}\left(\frac{\tau}{\tau^*}\right)^2, \tag{5}$$

which is validated numerically in Fig. 1; see the Supplemental Material [44]. Note that this exact result is consistent with our earlier scaling argument.

In order to validate the above scenario and to explore the effectiveness of the decoupling approximation in Eq. (4), we have performed numerical simulations for different dimensions. Very good agreement is observed for a wide range of parameters (see Fig. 2 for a two-dimensional infinite square lattice and [44] for the three-dimensional case). We show below that this approximation is actually exact in both limits $\rho \to 0$ (at linear order in ρ) and $\rho \to 1$.

Low-density limit.—In the dilute limit $\rho \to 0$, the system for the coefficients A_μ can be drastically simplified (see the Supplemental Material [44]). In this case, one has $A_\mu \sim 1 + (2d\tau^*/\tau)p_\mu$ and the TP velocity can be expressed as

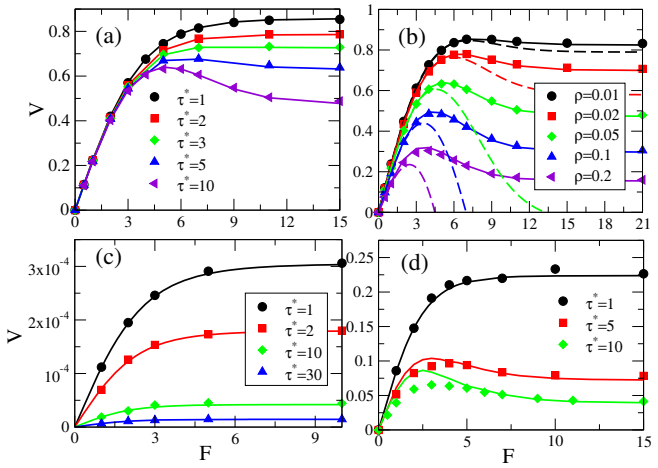

FIG. 2 (color online). $V(F)$ for $d = 2$ and $\beta = 1$: (a) $\rho = 0.05$, $\tau = 1$, and different τ^*, analytic prediction (lines) and numerical simulations (symbols); (b) $\tau = 1$ and $\tau^* = 10$, analytic prediction (continuous lines), numerical simulations (symbols), and linearized solution (dashed lines); (c) high-density limit, $\rho = 0.999$, with $\tau = 1$, and different τ^*, analytic prediction of Eq. (9) (lines) and numerical simulations (symbols); (d) $\rho = 0.5$, $\tau = 1$, and different τ^*, analytic prediction (lines) and numerical simulations (symbols).

$$V(\rho \to 0) = \frac{1}{\tau}(p_1 - p_{-1}) - \frac{\rho}{\tau}(p_1 - p_{-1} + p_1 v_1 - p_{-1} v_{-1}) + o(\rho), \quad (6)$$

where the coefficients $v_{\boldsymbol{n}}$ satisfy the linear system of equations

$$2d(1+\tau^*/\tau)v_{\boldsymbol{n}} = \sum_\nu [1 + (2d\tau^*/\tau)p_\nu] v_{\boldsymbol{e}_\nu} \nabla_{-\nu} \mathcal{F}_{\boldsymbol{n}} - (2d\tau^*/\tau)(p_1 - p_{-1})(\nabla_1 - \nabla_{-1})\mathcal{F}_{\boldsymbol{n}}. \quad (7)$$

Here, the functions $\mathcal{F}_{\boldsymbol{n}}$ depend on the coefficients A_μ, on the dimension of the system, and are reported explicitly in the Supplemental Material [44], while ∇_μ is a differential operator defined by the relation $\nabla_\mu f(\boldsymbol{\lambda}) \equiv f(\boldsymbol{\lambda} + \boldsymbol{e}_\mu) - f(\boldsymbol{\lambda})$. The $V(F)$ obtained in this dilute limit is reported in Fig. 2(b) (dashed lines) for different densities and shows the same behavior as the complete solution, even at intermediate values of ρ, for small enough forces.

A further simplification occurs in the limit considered in Ref. [33] of the standard Lorentz gas, namely when $\tau^*/\tau \to \infty$. In this case, from Eq. (7) we obtain an explicit solution, which actually coincides with the analytic results presented in [33]. In the particular case $d = 2$, the functions $\mathcal{F}_{\boldsymbol{n}}$ simplify to

$$\mathcal{F}_{\boldsymbol{n}} = e^{-n_1 F/2} \int_0^\infty e^{-t} I_{n_1}(2t/Z) I_{n_2}(2t/Z) dt, \quad (8)$$

with $I_n(x)$ the modified Bessel function of the first kind and $Z = 2 + e^{\beta F/2} + e^{-\beta F/2}$. Substituting Eq. (8) into the system (7), and using Eq. (6), one recovers the exact result of Ref. [33] (see the Supplemental Materal [44]). As the accuracy of our analytic results increases when τ^*/τ decreases, as shown numerically in Fig. 2, we claim that our decoupling approximation, Eq. (4), is exact at linear order in ρ.

High density limit.—As detailed in the Supplemental Material [44] and illustrated here in the particular case $d = 2$, the system for the coefficients A_μ linearized around $1 - \rho$ leads to

$$V(F) = \frac{1}{\tau}(1-\rho)\frac{\sinh(\beta F/2)}{1 + \cosh(\beta F/2)[1 + \frac{2\tau^*}{\tau}(\pi - 2)]}. \quad (9)$$

This result gives back the exact expression obtained in Ref. [40] in the particular case $\tau = \tau^*$.

Conclusion.—We have presented an analytic theory for NDM in a general driven lattice gas. Exploiting a decoupling approximation, we have obtained an analytic expression for the force-velocity relation. This expression which goes beyond linear response, is shown to be exact in both $\rho \to 0$ and $\rho \to 1$ regimes and turns out to be in very good agreement with numerical simulations for a wide range of parameters. In particular, for values of τ^* large enough, a nonmonotonic behavior of the TP velocity as a function of the external force is indeed observed. Our study extends analytical results obtained in Ref. [33] and sheds light on recent numerical observations [34,35]. In particular, with the choice of transition rates of Ref. [35], which do not depend on the field in the transverse direction, NDM is observed only for much larger values of τ^*/τ. This is due to the fact that the escape time of the TP from traps, in that case, is insensitive to the applied force to linear order in ρ.

Our solution reveals and quantifies a minimal physical mechanism responsible for NDM, which is based on the coupling between the density of obstacles and the diffusion time scales of the TP and obstacles. Our minimal model, which takes into account the repulsive part of the particle-particle interactions only, suggests that the phenomenon of the negative differential mobility should be a generic feature of biased transport in crowded environments.

The work of O. B. and A. S. is supported by the European Research Council (Grant No. FPTOpt-277998).

[1] U. Marini Bettolo Marconi, A. Puglisi, L. Rondoni, and A. Vulpiani, Phys. Rep. **461**, 111 (2008).
[2] L. Cugliandolo, J. Phys. A **44**, 483001 (2011).
[3] U. Seifert, Rep. Prog. Phys. **75**, 126001 (2012).
[4] G. Gradenigo, A. Puglisi, A. Sarracino, D. Villamaina, and A. Vulpiani, in *Nonequilibrium Statistical Physics of Small Systems: Fluctuation Relations and Beyond*, edited by R. Klages, W. Just, and C. Jarzynski (Wiley-VCH, Weinheim, 2012).
[5] A. Morita, Phys. Rev. A **34**, 1499 (1986).
[6] J.-P. Bouchaud and G. Biroli, Phys. Rev. B **72**, 064204 (2005).
[7] E. Lippiello, F. Corberi, A. Sarracino, and M. Zannetti, Phys. Rev. B **77**, 212201 (2008); Phys. Rev. E **78**, 041120 (2008).
[8] G. Diezemann, Phys. Rev. E **85**, 051502 (2012).
[9] O. Bénichou, P. Illien, G. Oshanin, and R. Voituriez, Phys. Rev. E **87**, 032164 (2013).
[10] P. Illien, O. Bénichou, C. Mejia-Monasterio, G. Oshanin, and R. Voituriez, Phys. Rev. Lett. **111**, 038102 (2013).
[11] O. Bénichou, A. Bodrova, D. Chakraborty, P. Illien, A. Law, C. Mejia-Monasterio, G. Oshanin, and R. Voituriez, Phys. Rev. Lett. **111**, 260601 (2013).
[12] P. Habdas, D. Schaar, A. C. Levitt, and E. R. Weeks, Europhys. Lett. **67**, 477 (2004).
[13] T. M. Squires and T. G. Mason, Annu. Rev. Fluid Mech. **42**, 413 (2010).
[14] L. G. Wilson, A. W. Harrison, A. B. Schofield, J. Arlt, and W. C. K. Poon, J. Phys. Chem. B **113**, 3806 (2009).
[15] D. J. Evans and G. Morriss, *Statistical Mechanics of Non-equilibrium Liquids* (Cambridge University Press, Cambridge, England, 2008).
[16] N. J. Wagner and J. F. Brady, Phys. Today **62**, No. 10, 27 (2009).

[17] R. K. P. Zia, E. L. Praestgaard, and O. G. Mouritsen, Am. J. Phys. **70**, 384 (2002).
[18] E. Conwell, Phys. Today **23**, No. 6, 35 (1970).
[19] F. Nava, C. Canali, F. Catellani, G. Gavioli, and G. Ottaviani, J. Phys. C **9**, 1685 (1976).
[20] C. J. Stanton, H. U. Baranger, and J. W. Wilkins, Appl. Phys. Lett. **49**, 176 (1986).
[21] X. L. Lei, N. J. M. Horing, and H. L. Cui, Phys. Rev. Lett. **66**, 3277 (1991).
[22] H. Böttger and V. V. Bryksin, Phys. Status Solidi B **113**, 9 (1982).
[23] See, e.g., S. B. Vrhovac and Z. Lj. Petrovic, Phys. Rev. E **53**, 4012 (1996).
[24] G. Benenti, G. Casati, T. Prosen, and D. Rossini, Europhys. Lett. **85**, 37001 (2009).
[25] G. W. Slater, H. L. Guo, and G. I. Nixon, Phys. Rev. Lett. **78**, 1170 (1997).
[26] M. Kostur, L. Machura, P. Hänggi, J. Luczka, and P. Talkner, Physica (Amsterdam) **371A**, 20 (2006).
[27] R. Eichhorn, J. Regtmeier, D. Anselmetti, and P. Reimann, Soft Matter **6**, 1858 (2010).
[28] R. L. Jack, D. Kelsey, J. P. Garrahan, and D. Chandler, Phys. Rev. E **78**, 011506 (2008).
[29] M. Sellitto, Phys. Rev. Lett. **101**, 048301 (2008).
[30] F. Turci, E. Pitard, and M. Sellitto, Phys. Rev. E **86**, 031112 (2012).
[31] T. Chou, K. Mallick, and R. K. P. Zia, Rep. Prog. Phys. **74**, 116601 (2011).
[32] M. Barma and D. Dhar, J. Phys. C **16**, 1451 (1983).
[33] S. Leitmann and T. Franosch, Phys. Rev. Lett. **111**, 190603 (2013).
[34] P. Baerts, U. Basu, C. Maes, and S. Safaverdi, Phys. Rev. E **88**, 052109 (2013).
[35] U. Basu and C. Maes, J. Phys. A **47**, 255003 (2014).
[36] E. Lippiello, F. Corberi, and M. Zannetti, Phys. Rev. E **71**, 036104 (2005).
[37] M. Baiesi, C. Maes, and B. Wynants, Phys. Rev. Lett. **103**, 010602 (2009).
[38] O. Bénichou, A. M. Cazabat, J. De Coninck, M. Moreau, and G. Oshanin, Phys. Rev. Lett. **84**, 511 (2000).
[39] O. Bénichou, A. M. Cazabat, J. De Coninck, M. Moreau, and G. Oshanin, Phys. Rev. B **63**, 235413 (2001).
[40] O. Bénichou and G. Oshanin, Phys. Rev. E **66**, 031101 (2002).
[41] Let us note that the change of behavior observed in the model does not represent a genuine phase transition occurring in the system.
[42] J. L. Lebowitz and H. Spohn, J. Stat. Phys. **95**, 333 (1999).
[43] The choice of transition rates studied in Ref. [35] corresponds to taking, for $d = 2$, $p_1 = (1/2)e^{\beta F/2}/(e^{\beta F/2} + e^{-\beta F/2})$, $p_{-1} = (1/2)e^{-\beta F/2}/(e^{\beta F/2} + e^{-\beta F/2})$ and $p_2 = p_{-2} = 1/4$, with $\tau = 1/2$ and $\tau^* = 1/4\gamma$, where γ is the inverse time scale introduced in [35].
[44] See Supplemental Material at http://link.aps.org/supplemental/10.1103/PhysRevLett.113.268002, which includes Ref. [45], for details on the calculations and numerical simulations.
[45] B. D. Hughes, *Random Walks and Random Environments* (Oxford Science, Oxford, 1995).
[46] S. F. Burlatsky, G. Oshanin, M. Moreau, and W. P. Reinhardt, Phys. Rev. E **54**, 3165 (1996).